removal of atomic hydrogen, since reaction 1 is very slow and the experiment required long reaction time.

Discussion

Comparison with Previous Works. There appears to be a large discrepancy in the branching fractions for (2a) and (2b); von Aders and Wagner[1] neglected the consumption of ketene by reaction 5; the analysis in the experiment performed by Slemr and Warneck[2] included a large correction for reaction 5. However the rate constant they used for reaction 5 was about twice as large as the recent measurement. Thus we reanalyzed the values of previous measurements using the recent rate constant for reaction 5. The results are also shown in Table I. Better agreement with the present work is thereby obtained.

The present rate constant for reaction 1 agrees with those of the previous measurements,[3,4] though it contains large uncertainty.

Comparison with Analogous Systems. Analogous product branching of radical atom reactions with reaction 2 is known for several systems. The reaction of CH_3CO with atomic oxygen proceeds via two pathways:

$$CH_3CO + O \rightarrow CH_3 + CO_2 \qquad (16a)$$

$$\rightarrow CH_2CO + OH \qquad (16b)$$
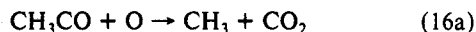
and the branching fractions have been determined to be $76 \pm 24\%$ and $22 \pm 5\%$, respectively.[7] Reaction of a smaller carbonyl radical,

HCO, with hydrogen atoms has been investigated theoretically[8] and revealed to proceed via two pathways (an addition–elimination pathway, (17a), and a direct abstraction pathway, (17b)):

$$HCO + H \rightarrow (H_2CO)^* \rightarrow H_2 + CO \qquad (17a)$$

$$\rightarrow H_2 + CO \qquad (17b)$$
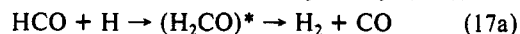
with almost equal branching fractions (45% and 55% for (17a) and (17b), respectively).

Although no theoretical information on the reaction dynamics has been available for reactions 2 and 16, reactions 2a and 16a will be addition–elimination processes similar to reaction 17a and reactions 2b and 16b will be direct abstractions similar to reaction 17b. Though one might consider that reactions 2b and 16b are addition–elimination processes, the elimination processes will be entropically unfavorable because the methyl group intramolecular rotation is restricted at the transition state. This effect has been quantitatively discussed on $C_2H_5 + O$ system.[9] Therefore, reactions 2b and 16b will be direct abstractions. This type of reaction (one bond breaks and two bonds are formed via reaction) usually has no (or a very small) barrier on potential energy surfaces and easily occur even at room temperature. For more reliable discussion on the reaction dynamics, an ab initio calculation of the potential energy surfaces of these reactions are needed.

(5) Washida, N.; Hatakeyama, S.; Takagi, H.; Kyogoku, T.; Sato, S. *J. Chem. Phys.* **1983**, *78*, 4533.
(6) Michael, J. V.; Nava, D. F.; Payne, W. A.; Stief, L. J. *J. Chem. Phys.* **1979**, *70*, 5222.

(7) Miyoshi, A.; Matsui, H.; Washida, N. *J. Phys. Chem.* **1989**, *93*, 5813.
(8) Harding, L. B.; Wagner, A. F. *Symp. (Int.) Comust., [Proc.], 21st* **1986**, 721.
(9) Slagle, I. R.; Sarzyński, D.; Gutman, D.; Miller, J. A.; Melius, C. F. *J. Chem. Soc., Faraday Trans. 2* **1988**, *84*(5), 491.

Heterogeneous Reactions on Model Polar Stratospheric Cloud Surfaces: Reaction of N2O5 on Ice and Nitric Acid Trihydrate
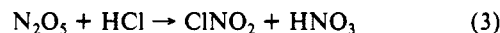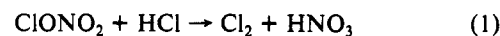
Michael A. Quinlan,†　Christa M. Reihs,‡　David M. Golden, and Margaret A. Tolbert*

Chemical Kinetics Department, SRI International, Menlo Park, California 94025 (Received: October 18, 1989; In Final Form: February 12, 1990)

A Knudsen cell flow reactor was used to study the heterogeneous reaction of N_2O_5 on laboratory ice surfaces and nitric acid trihydrate (NAT) surfaces representative of polar stratospheric clouds (PSCs). N_2O_5 was quantitatively converted to HNO_3 on ice surfaces at 188 K. On initially pure ice surfaces, a gradual increase in the N_2O_5 uptake efficiency was observed up to a maximum value near 0.03. The slow rise in reactivity with time is consistent with an acid-catalyzed surface reaction. With increasing initial nitric acid concentrations, the maximum reactivity occurred more rapidly although the overall reactivity was depressed. The uptake efficiency for N_2O_5 on NAT at 188 K was found to be 0.015 ± 0.006.

Introduction

Heterogeneous reactions on the surfaces of polar stratospheric clouds (PSCs) over Antarctica are now recognized to play a central role in the photochemical mechanism responsible for the dramatic yearly occurrence of the Antarctic "ozone hole".[1] Laboratory studies[2-6] have confirmed that heterogeneous reactions can occur on ice surfaces thought to be representative of type II PSCs found in the cold Antarctic stratosphere. For example, reactions 1–3 involving reactive chlorine have been shown to occur readily on laboratory ice surfaces. These reactions convert the stable chlorine reservoir species ($ClONO_2$ and HCl) into more active forms ($HOCl$, Cl_2, $ClNO_2$) which photolyze readily to provide Cl for catalytic ozone destruction cycles.[7]

$$ClONO_2 + HCl \rightarrow Cl_2 + HNO_3 \qquad (1)$$

$$ClONO_2 + H_2O \rightarrow HOCl + HNO_3 \qquad (2)$$

$$N_2O_5 + HCl \rightarrow ClNO_2 + HNO_3 \qquad (3)$$

The fate of odd nitrogen in the Antarctic stratosphere is also of key importance in understanding the ozone losses observed there. All of the above reactions plus reaction 4 result in the formation

$$N_2O_5 + H_2O \rightarrow 2HNO_3 \qquad (4)$$

† Current address: Department of Chemistry, University of California, Berkeley, CA 94720.
‡ Postdoctoral Research Associate.

(1) Solomon, S. *Rev. Geophys.* **1988**, *26*, 131.
(2) Molina, M. J.; Tso, T.-L.; Molina, L. T.; Wang, F. C.-Y. *Science* **1987**, *238*, 1253.
(3) Tolbert, M. A.; Rossi, M. J.; Malhotra, R.; Golden, D. M. *Science* **1987**, *238*, 1258.
(4) Tolbert, M. A.; Rossi, M. J.; Golden, D. M. *Science* **1988**, *240*, 1018.
(5) Leu, M.-T. *Geophys. Res. Lett.* **1988**, *15*, 17.
(6) Leu, M.-T. *Geophys. Res. Lett.* **1988**, *15*, 851.
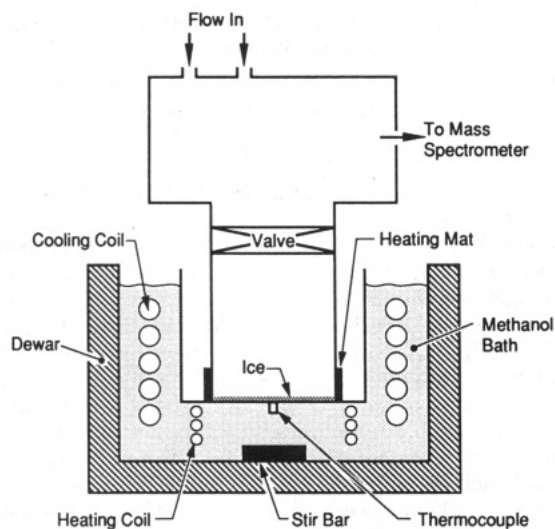(7) Molina, L. T.; Molina, M. J. *J. Phys. Chem.* **1987**, *91*, 433.

Figure 1. Schematic diagram of the Knudsen cell flow reactor.

of nitric acid. On laboratory ice surfaces at 188 K, the nitric acid is retained in the condensed phase. On PSCs, particle evaporation could lead to enhanced levels of gas-phase HNO_3. Ultimately, the conversion of odd nitrogen to nitric acid has two important consequences. First, the resulting low levels of NO_2 preclude the sequestering of active chlorine. Second, high levels of nitric acid may promote the formation of type I PSCs, thought to be composed of mixtures of nitric acid and ice. Type I PSCs may themselves provide active sites for catalytic reactions such as (1)–(4).

Type I PSCs have recently been characterized by field measurements[8] as well as laboratory studies[9,10] and model calculations.[11] These studies indicate that type I PSCs are nitric acid trihydrate (NAT) crystals (or solid solutions of nitric acid in ice) which form in the Antarctic stratosphere at temperatures 5–7 K higher than the frost point. Because they can form at warmer temperatures, type I PSCs may also form in the winter Arctic stratosphere, where temperatures are rarely low enough to support the formation of type II PSCs (ice). Recent results have indicated that, like the situation over Antarctica, the Arctic stratosphere may undergo severe chemical perturbation during the cold winter months.[12,13] As well as these field studies, models suggest that heterogeneous interactions at high northern latitudes in the winter could lead to chemical perturbations.[14,15] A recent study has suggested that type I PSCs may even be able to form near the tropopause at tropical latitudes.[16]

In order to assess the importance of heterogeneous reactions 1–4 on type I PSCs, laboratory studies are needed to determine the uptake efficiencies. In this paper we present a study of reaction 4 on a series of ice and nitric acid/ice surfaces at stratospheric temperatures. We have previously studied reaction 4 on pure ice surfaces and determined an uptake efficiency of >0.001.[4] In the present study, we have used an improved apparatus to more accurately measure the uptake efficiency. In addition, we have included surfaces containing both nitric acid and ice approaching a 3:1 mixture of H_2O/HNO_3. The reaction of N_2O_5 on these

TABLE I: Simplified Kinetic Scheme for the Reaction of a Gas on a Surface in a Knudsen Cell

process	rate	description
$\rightarrow G$	F^i	flow in
$G + S \rightarrow G{\cdot}S$	$k_{trap}[G][S]$	trapping
$G{\cdot}S \rightarrow G + S$	$k_{evap}[G{\cdot}S]$	evaporation
$G{\cdot}S \rightarrow$ products	$k_{rxn}[G{\cdot}S]$	reaction
$G \rightarrow$	$k_e[G]$	escape to mass spectrometer

surfaces will be compared in order to identify similarities and differences in the reactivities of type I and type II PSCs.

Experimental Section

The reaction of N_2O_5 on ice and NAT surfaces was studied by using an improved version of a Knudsen cell flow reactor described previously.[17] A schematic diagram of the current apparatus is shown in Figure 1. Briefly, the Knudsen cell consists of two Pyrex chambers separated by a valve. The ice surfaces are formed in the lower chamber which is immersed in a cold methanol bath regulated to the desired temperature by a combination of liquid nitrogen cooling and resistive heating. The upper chamber is coupled to a differentially pumped mass spectrometer through an escape orifice with variable area. The mass spectrometer intensity for a given molecule is proportional to its flux, F (molecules/s), out of the Knudsen cell. Reactant gases are initially routed through the upper chamber, bypassing the cold ice surface. Changes in the mass spectrometer signal that occur when the valve is opened measure the flux of reactant gas that is lost to the cold surface. Condensed-phase products are determined subsequently by slowly warming (3 K/min) the surface and monitoring the partial pressures of the adsorbed species as the ice evaporates. In the present study, N_2O_5 is monitored using mass peaks 30 and 46 and HNO_3 is monitored using mass peaks 30, 46, and 63. The mass spectrometric data and reactor temperature are acquired from a microcomputer. Data for ionic mass fragments at m/e 18, 30, 46, and 63 are collected at intervals of one mass set every 5 s.

The experimental quantity that is measured in the present work is the net uptake efficiency for N_2O_5, γ, defined by eq 5. The

$$\gamma = \frac{\text{no. of reactant molecules lost (molecules/s)}}{\text{no. of gas–surface collisions (collisions/s)}} \quad (5)$$

number of reactant molecules lost is measured in our Knudsen cell as the quantity $(F^0 - F)$ where F^0 and F are the reactant fluxes (molecules/s) out of the cell in the absence and presence of the ice surface, respectively. The total gas–surface collision frequency, ω (collisions/s) is obtained from kinetic theory as

$$\omega = \frac{1}{4}\langle v \rangle A_s(N/V) \quad (6)$$

where $\langle v \rangle$ is the average molecular velocity (cm/s), A_s is the area of the surface (cm^2), and N/V is the reactant gas number density (molecules/cm^3). The number density in a Knudsen cell is simply related to the reactant flux, F, and the size of the escape orifice, A_h, by

$$N/V = 4F/A_h\langle v \rangle \quad (7)$$

The net uptake efficiency is easily obtained combining eqs 5–7 and is given by

$$\gamma = A_h/A_s[(F^0 - F)/F] \quad (8)$$

The net uptake efficiency may describe a sequence of events.[18,19] For example, the reaction sequence in Table I is a possible scheme

(8) Fahey, D. W.; Kelly, K. K.; Ferry, G. V.; Poole, L. R.; Wilson, J. C.; Murphy, D. M.; Loewenstein, M.; Chan, K. R. *J. Geophys. Res.* **1989**, *94*, 11, 299.

(9) Hanson, D.; Mauersberger, K. *J. Phys. Chem.* **1988**, *92*, 6167.

(10) Hanson, D.; Mauersberger, K. *Geophys. Res. Lett.* **1988**, *15*, 855.

(11) Turco, R. P.; Toon, O. B.; Hamill, P. *J. Geophys. Res.* **1989**, *94*, 16493.

(12) Solomon, S.; Mount, G. H.; Sanders, R. W.; Jakoubek, R. O.; Schmeltekopf, A. L. *Science* **1988**, *242*, 550.

(13) Mount, G. H.; Solomon, S.; Sanders, R. W.; Jakoubek, R. O.; Schmeltekopf, A. L. *Science* **1988**, *242*, 555.

(14) Austin, J.; Garcia, R. R.; Russell, J. M., III; Solomon, S.; Tuck, A. F. *J. Geophys. Res.* **1986**, *91*, 5477.

(15) Douglass, A. R.; Stolarski, R. S. *Geophys. Res. Lett.* **1989**, *16*, 131.

(16) Hamill, P.; Fiocco, G. *Geophys. Res. Lett.* **1988**, *15*, 1189.

(17) Golden, D. M.; Spokes, G. N.; Benson, S. W. *Angew. Chem., Int. Ed. Engl.* **1973**, *12*, 534.

(18) Schwartz, S. E. In *Chemistry of Multiphase Atmospheric Systems*; NATO ASI Series; Jaeschke, W., Ed.; Springer-Verlag: Berlin, 1986; Vol. G6.

(19) Boudart, M.; Djega-Mariadassou, G. *Kinetics of Heterogeneous Catalytic Reactions*; Princeton University Press: Princeton, NJ, 1984.

to describe a gas–surface reaction in our Knudsen cell apparatus. In this set of reactions, G represents a gas-phase molecule, S an available surface site, and G·S a molecule trapped in a precursor state on the surface. Molecules trapped in a precursor state can either react on the surface to form products or evaporate back to the gas phase. The pseudo-first-order rate constant for trapping, $k_{trap}[S]$, is given by $\alpha\omega$ where α is the "trapping" efficiency. (In the literature, one often sees both α and γ referred to as the "sticking coefficient". We have avoided this nomenclature.) If one applies a steady-state analysis to the equations in Table I, eq 9 is obtained, where $[G^0]$ and $[G]$ are the steady-state con-

$$\{([G^0] - [G])/[G]\}A_h/A_s = \gamma = \alpha[k_{rxn}/(k_{evap} + k_{rxn})] \qquad (9)$$

centrations of G in the absence and presence of the surface, respectively. It can be seen that $\gamma = \alpha$ only for the case where no reevaporation occurs. When there is no barrier to adsorption via a precursor state, α is often taken to be unity. For systems where reevaporation does occur, our measured uptake efficiency is always less than the trapping efficiency.[18,20]

In the present study, we measure the vapor pressure of the surface after the experiments to monitor evaporation. For ice and NAT surfaces, we see no m/e 46 signal after the experiments, suggesting little long-term N_2O_5 or HNO_3 evaporation. Furthermore, the measured yield of condensed HNO_3 near 100% (see below) suggests that little HNO_3 is evaporating on any time scale. However, rapid N_2O_5 evaporation (faster than the experimental time scale of seconds) probably is occurring, making the measured uptake efficiencies less than unity.

The uptake efficiency need not be constant in time. In fact, it is the exception, rather than the rule, to obtain time-invariant values for γ. A variation in γ with time is a direct reflection of changes that occur on the surface as the heterogeneous interaction proceeds. For example, if the adsorbate or its decomposition products build up on the surface, the number of available surface sites will be lowered, and the measured uptake efficiency will be depressed. Surface saturation will ultimately lead to an uptake efficiency of zero. In the present study, we do in fact observe time-dependent values for γ. Possible reasons for this will be discussed in more detail later.

In our current apparatus, we have modified the reactor parameters to allow the measurement of relatively large values for γ. By use of two escape orifices (A_h = 0.2 and 0.05 cm²) and two different surface area reactors (A_s = 10 and 40 cm²), values of A_h/A_s ranging from 0.02 to 0.001 are obtained. With these ratios, we estimate that uptake efficiencies in the range (0.2–1) × 10⁻⁴ can be accurately determined. We have been able to measure quite large uptakes in several cases. For example, uptake efficiencies in the range 0.2–0.3 were measured for both HCl and H_2O on pure ice surfaces.[21]

The determination of γ using eq 8 relies heavily on an accurate determination of the ice surface area. Although the geometric surface area of the current reactor is well known, there may be substantial errors in the total available surface area due to microscopic structure on the ice surface. For example, BET (Brunauer, Emmett, and Teller)[19] surface area measurements have shown that ice[22] and NAT[23] have microscopic surface areas on the order of 10⁴ cm²/g. Previous studies have shown that for large uptake efficiencies, the uptake is almost independent of the microscopic surface area.[24] For γ < 0.01, the microscopic surface area is likely to contribute. Future work will attempt to measure BET surface areas of our ice in situ for more accurate absolute values of γ. For the current study, we have tried to minimize the problem of microscopic surface structure by studying ice surfaces prepared in different ways as described below. The surface area

used in eq 8 is the geometric surface area.

The ice and NAT surfaces used in the present study were made in two ways. "Bulk" surfaces were obtained by slowly (100 K in 1 h) freezing 10–40 mL of water or mixtures of nitric acid in water. The exact surface composition of these solids is not known and can only be estimated based on the starting bulk concentration. All of the bulk samples, studied at temperatures from 188 to 198 K, appeared to be frozen solid and were somewhat irregular in appearance. While bulk ice appeared glassy, bulk NAT appeared white and crystalline. "Film" surfaces were obtained by co-condensing water and nitric acid onto the reactor at low temperature. The calculated thicknesses of the films ranged from 5000 to 50 000 layers.

The solids used in the present study were characterized by their vapor pressures. Note that vapor pressure measurements do not provide a complete identification of the surfaces. Work in progress in our laboratory is aimed at better characterizing the surfaces using *in situ* FTIR analysis. Vapor pressures are measured in the Knudsen cell by turning off all incoming flows and measuring the flux out of the Knudsen cell from the surface alone. Equation 7 can then be used to determine the gas number density. We measure water vapor pressures near 7 × 10⁻³ Torr at 213 K and near 2.5 × 10⁻³ Torr at 203 K for pure ice. Within experimental uncertainty (±50%) the water vapor pressure over NAT was the same as over pure ice. No nitric acid was detected over any of the nitric acid/ice surfaces used at 198 or 188 K, indicating a partial pressure less than 10⁻⁶ Torr.

For bulk ice and bulk NAT surfaces, experiments were sometimes performed with water added to the reactor during the exposure of the surface to N_2O_5. The water was added to exactly compensate for the water removed from the surface due to slow pumping on the surface through the escape orifice. For example, assuming a water vapor pressure of 4.5 × 10⁻⁴ Torr and a pumping speed through the escape orifice of 3 × 10³ cm³/s, we estimate that the surface loses 4 × 10³ layers/h (or 2 μm/h) due to evaporation. No qualitative differences were observed in the behavior of the N_2O_5 uptake efficiency on either bulk ice or bulk NAT when water was added during the reaction relative to no water addition. Although the exact value for γ did show some variation, it was within the quoted uncertainty of the experiment.

Results and Discussion

Reactivity of N_2O_5 on Ice Surfaces. Typical results for the heterogeneous interaction of N_2O_5 on a thin ice film (5000 layers) are shown in Figure 2. In part a, the mass spectrometer signal for mass 46 is shown as the valve is opened to expose the ice film to N_2O_5. The flux of N_2O_5 to the surface was 4.7 × 10¹⁴ molecules/(cm² s). After opening the valve, the mass 46 signal slowly drops due to loss of N_2O_5 on the ice surface. After ∼125 s, the signal rises again to an apparent steady-state value. The signal returns to the original level when the valve is closed after exposure. The exact behavior of the signal critically depends on the flux of N_2O_5 to the surface. In general, the induction period required to attain the minimum signal rapidly decreases with increasing N_2O_5 flux to the surface (see below).

The possibility of gas-phase products was investigated. No gaseous nitric acid was observed as evidenced by the lack of mass 63, the parent fragment ion for HNO_3. In addition, there was no evidence for either NO or NO_2 formation. This was determined by monitoring the ratio of mass 46/30 as the valve was opened and closed (Figure 2b). Whereas the mass 46/30 ratio for N_2O_5 is near 2.0, NO_2 and NO have mass 46/30 ratios of 0.4 and 0.0, respectively. Although the mass 46 signal changed greatly as the reaction proceeded (Figure 2a), the ratio of mass 46/30 remained remarkably constant, suggesting that neither NO nor NO_2 was formed in quantities larger than 15%. The mass 46 signal observed in Figure 2a is therefore assumed to be entirely due to gaseous N_2O_5.

With this assumption, the change in signal in Figure 2a reflects the amount of N_2O_5 that is lost to the surface at any given point in time. The uptake efficiencies can then be determined by using this data in conjunction with eq 8. This is shown in Figure 2c,

(20) Worsnop, D. R.; Zahniser, M. S.; Kolb, C. E.; Gardner, J. A.; Watson, L. R.; Van Doren, J. M.; Jayne, J. T.; Davidovits, P. *J. Phys. Chem.* **1989**, *93*, 1159.

(21) Tolbert, M. A.; et al. Unpublished results.

(22) Adamson, A. *Prog. Surf. Membr. Sci.* **1974**, *8*, 285.

(23) Moore, S. B.; Keyser, L. F.; Leu, M.-T.; Turco, R. P.; Smith, R. H. *Nature*, in press.

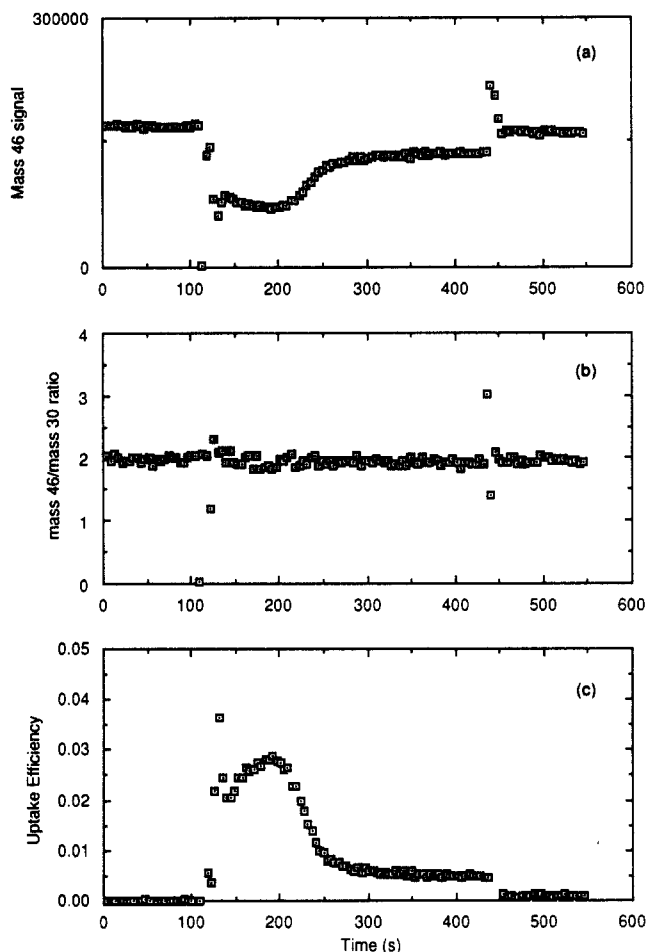(24) Davy, J. G.; Somorjai, G. A. *J. Chem. Phys.* **1971**, *55*, 3624.

Figure 2. Heterogeneous reaction of N_2O_5 on a thin ice film at 188 K. The valve is opened to expose the surface to N_2O_5 at $t = 110$ s and closed again at $t = 450$ s. The three panels for this single experiment indicate (a) the mass 46 signal, (b) the ratio of mass 46/30, and (c) the time varying uptake efficiencies calculated at each point via eq 8.

TABLE II: Flux Dependence of N_2O_5 Uptake by Ice

ice type	N_2O_5 flux, molecules/(cm^2 s)	N_2O_5 taken up by γ_{max}, molecules/cm^2
bulk	1.1×10^{14}	5×10^{16}
bulk	1.3×10^{14}	5×10^{16}
bulk	1.6×10^{14}	5×10^{16}
bulk	4.6×10^{14}	6×10^{16}
film	5.0×10^{13}	4×10^{16}
film	1.4×10^{14}	3×10^{16}
film	4.4×10^{14}	7×10^{16}
film	4.7×10^{14}	3×10^{16}
film	3.8×10^{14}	3×10^{16}

the absolute number of N_2O_5 molecules lost to the surface. For example, an 875-s exposure of N_2O_5 to film ice resulted in 8×10^{17} molecules being lost to the surface. The number of nitric acid molecules formed as a result of reaction 4 can be determined after the exposure by evaporating the ice film and monitoring mass peaks 30, 46, and 63 due to nitric acid. Calibration of nitric acid showed a linear relationship between the nitric acid flux and the intensities for these three mass peaks. Using the calibrations for mass peaks 30, 46, and 63, we calculated the amount of nitric acid recovered during evaporation as 1.56×10^{18}, 1.44×10^{18}, and 2.17×10^{18} molecules, respectively. These values correspond to yields for reaction 4 of 98%, 90%, or 135% depending on which mass is used (i.e., m/e 30, 46, or 63, respectively). The mass 63 signal from nitric acid is quite small, and thus the yield determined by using it is considered the least accurate. The above yields suggest that, within the experimental uncertainties, N_2O_5 is quantitatively converted to condensed-phase HNO_3 via reaction 4 on ice.

Although the product of reaction 4 is very clear, the time dependence of the uptake efficiency for this process is not. The 125-s rise to γ_{max} in Figure 2c is suggestive of an autocatalytic reaction whose rate increases as the reaction proceeds. Because HNO_3 is the only reaction product, this suggests that reaction 4 is acid catalyzed. This is not surprising when it is recognized that N_2O_5 in the condensed phase is thought to exist in ionic form, i.e., NO_2^+-NO_3^-.[26] Attack by acid at the negatively charged NO_3^- could lead to enhanced decomposition rates for N_2O_5. The ionic nature of this reaction on ice has been suggested previously[27] and has also been discussed in reference to the same reaction on sulfuric acid surfaces.[28] Another possible explanation for the apparent autocatalytic nature of reaction 4 on ice may be that nitric acid creates a defect on the ice surface, which makes the surrounding water molecules more reactive. Nitric acid in the ice lattice of single-crystal ice may be incorporated either substitutionally or interstitially,[29] creating an orientational defect in either case. The self-diffusion of water in ice and the electrical properties of ice are thought to be related to such orientational defects in the ice structure.[30] Thus, the increased reactivity as nitric acid is formed may be related to growing ice defects on the surface.

The fall in γ at longer times in Figure 2a is likely to be due to surface saturation. As the amount of nitric aid formed on the surface increases, the surface looks less and less like a pure ice surface. In fact, at longer times, it is likely that the surface composition is closer to NAT than to pure ice. Similar behavior has been seen for adsorption on single-crystal surfaces, where the uptake initially increases due to attractive interactions and then decreases due to saturation.[31] In what follows, we will attempt to rationalize the observed time-dependent data in a somewhat more quantitative way.

where the maximum value of γ is 0.03 and the apparent steady-state value is 0.004. Fifteen different experiments on ice surfaces were performed using various combinations of A_h and A_s. Seven experiments on bulk ice resulted in an averaged maximum uptake efficiency $\gamma_{max} = 0.034 \pm 0.008$ (1 standard deviation). Eight experiments on film ice resulted in a maximum uptake efficiency $\gamma_{max} = 0.023 \pm 0.008$. The observed differences between bulk and film ice may be related to differences in microscopic surface area of the ice. However, the differences measured are within the experimental uncertainties and may not be statistically significant.

The observed uptake efficiencies can be compared to studies from other laboratories. Leu[6] reports a value of $\gamma = 0.028$ for N_2O_5 on thick film ice using an ice-coated flow tube reactor at 195 K. Worsnop et al.[25] report an uptake efficiency of 0.08 for N_2O_5 on water droplets at a temperature of 273 K. It can be seen that our maximum value is in excellent agreement with Leu but is substantially lower than that of Worsnop et al. This value may be sensitive to variations in surface phase, reaction temperature, or time scale.

Previous studies in our laboratory have indicated that HNO_3 is retained in the ice as a result of reaction 4.[4] This is confirmed in the present study. As discussed above, the mass 46 signal during the exposure of N_2O_5 to ice is due entirely to N_2O_5. Calibrations using known fluxes of N_2O_5 result in a linear relationship between the N_2O_5 flux and the mass spectrometer signal for mass 46. We can thus use the decrease in mass spectrometer signal to determine

(25) Worsnop, D.; Zahniser, M.; Kolb, C.; Watson, L.; Van Doren, J.; Jayne, J.; Davidovits, P. Polar Ozone Workshop, NASA Conference Publication 10014, 1988; p 98.
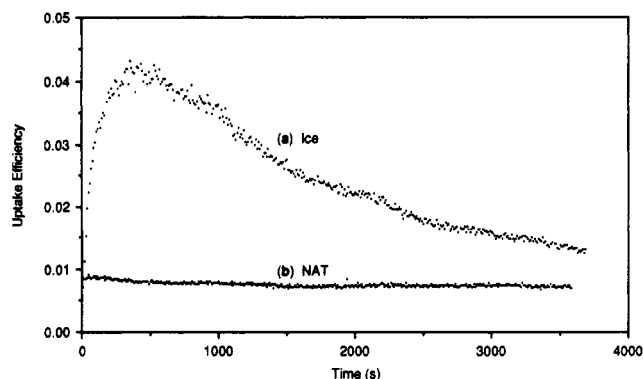
(26) Moeller, T. *Inorganic Chemistry*; Wiley: New York, 1952; p 608.
(27) Wofsy, S. C.; Molina, M. J.; Salawitch, R. J.; Fox, L. E.; McElroy, M. B. *J. Geophys. Res.* **1988**, *93*, 2442.
(28) Mozurkewich, M.; Calvert, J. G. *J. Geophys. Res.* **1988**, *93*, 15, 889.
(29) Elliott, S.; Turco, R. P.; Toon, O. B.; Hamill, P. *Geophys. Res. Lett.*, in press.
(30) Eisenberg, D.; Kauzmann, W. *The Structure and Properties of Water*; Oxford University Press: New York, 1969; p 121.
(31) King, D. A. In *Chemistry and Physics of Solid Surfaces*; Vanselow, R., Ed.; CRC Press: Boca Raton, FL, 1979; Vol. 2.

Figure 3. Comparison of the uptake efficiencies observed for N_2O_5 on (a) bulk ice versus (b) bulk NAT at 188 K. For both curves, water vapor was added to account for water removed from the surface due to pumping through the escape orifice.

As mentioned above, the time required to attain the maximum γ is a function of N_2O_5 flux to the surface. For example, curve a in Figure 3 displays the uptake of N_2O_5 by bulk ice using an N_2O_5 flux of 1.1×10^{14} molecules/(cm^2 s), approximately 4 times lower than the flux used in Figure 2c. It can be seen that although γ_{max} is similar for the two cases, the time to reach γ_{max} is longer for the lower flux. Thus, the total amount of N_2O_5 adsorbed by the time of maximum reactivity is quite similar in the two cases. This can be quantified by calculating the integrated number of N_2O_5 molecules lost to the surface by the time of γ_{max}. This is summarized in Table II. It can be seen that varying the N_2O_5 flux by almost an order of magnitude makes very little difference in the total amount of N_2O_5 taken up by the time of maximum reactivity. The average amount of N_2O_5 taken up by the time of maximum reactivity is 4.6×10^{16} molecules/cm^2. This corresponds to 9.2×10^{16} molecules/cm^2 of HNO_3 on the surface. A typical value for a monolayer coverage on a single-crystal surface is near 1×10^{15} molecules/cm^2. Thus, by the time of maximum reactivity, the observed nitric acid coverage is almost 100 times larger than monolayer coverage. This suggests that the actual surface area available for nitric acid adsorption is much larger than the geometrical surface area. There are several possible explanations for this.

The larger effective surface area could indicate that long-range attractive forces result in more than monolayer surface coverage of HNO_3. Alternatively, surface diffusion of N_2O_5 along the ice surface or along grain boundaries could allow the N_2O_5 to sample more surface area than the geometric area before either reacting or evaporating. Finally, some portion of the microscopic surface area might be exposed to the reactive gases and thus available for reaction. Recall that the microscopic surface area of ice has been estimated to be near 10^4 cm^2/g. Note, however, that the amount of N_2O_5 taken up by a thin (5000 layer) film is very close to the amount taken up by a thick (0.5 cm) bulk sample. It is therefore clear that the N_2O_5 does not sample the entire microscopic ice surface area. Rather, the available surface area appears to be somewhere between the geometric and microscopic surface areas. Future work will attempt to quantify the amount of surface probed during our gas adsorption experiments. Gas adsorption measurements as a function of film thicknesses should also provide clues to the effective surface areas.

Reactivity of N_2O_5 on NAT Surfaces. The uptake efficiency for N_2O_5 on a bulk 0.20 mole fraction HNO_3 ice is shown as curve b in Figure 3. We will refer to this solid as NAT, even though the stoichiometry and vapor pressures suggest that it may in fact be a mixture of ice and NAT.[9,10] The N_2O_5 flux to the surface is 1.1×10^{14} molecules/(cm^2 s), the same value as for curve a of Figure 3. The early time behavior is quite different in the case of N_2O_5 on NAT versus ice. Whereas the uptake efficiency of N_2O_5 on the ice surface slowly rises to a maximum value near 0.04, the uptake efficiency on NAT rapidly reaches a constant, but lower, value near $\gamma = 0.01$. Twelve different experiments on bulk and film surfaces using various combinations of A_h and A_s
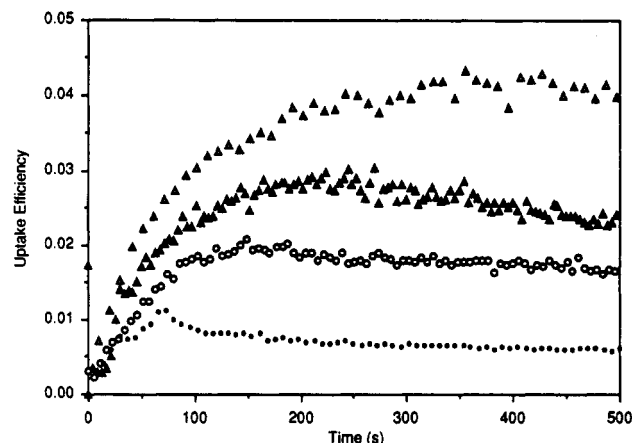

Figure 4. Variation in the time dependence of the observed uptake efficiencies for N_2O_5 on ice surfaces containing nitric acid. The bulk surfaces had the following initial compositions: $\triangle$, pure ice; $\blacktriangle$, 2.5×10^{-4} M HNO_3; O, 2.5×10^{-2} M HNO_3; $\bullet$, 0.25 M HNO_3.

resulted in an average value of $\gamma = 0.015 \pm 0.006$ for N_2O_5 on NAT surfaces. One of the 12 samples had a quite high value of $\gamma = 0.03$. Neglecting this value results in $\gamma = 0.013 \pm 0.003$ for the remaining 11 experiments. The experiment shown in curve b of Figure 3 represents the lowest value observed on NAT and was chosen for comparison with curve a because identical conditions were used. There was no statistical difference between the reactivity of bulk versus film NAT surfaces. From Figure 3, it can be seen that for long exposure times the reactivity of ice approaches that of NAT. This suggests that buildup of nitric acid on the ice surface slowly converts it into a surface that resembles NAT.

Reactivity of N_2O_5 on Other Nitric Acid/Ice Surfaces. Because reaction 4 appeared to be autocatalytic on ice, we assumed that adding very small amounts of HNO_3 to the ice prior to reaction would result in an enhanced uptake of N_2O_5 at early times. We thus studied the reaction of N_2O_5 on a series of substrates prepared from solutions containing nitric acid concentrations ranging from 2.5×10^{-4} to 0.25 M. To obtain the best comparison between the different solutions, all were studied with the same reactor size, escape orifice size, sample temperature, and sample volume. The observed γ values as a function of time are plotted in Figure 4.

It can be seen that surfaces prepared from initially acidic solutions of nitric acid have lower absolute values for γ_{max}. Note that although these are plots of individual experiments with fairly large uncertainties in γ (see above), the observed trends are certainly very suggestive. Even addition of very small amounts of HNO_3 (i.e., 2.5×10^{-4} M HNO_3) appear to quench the uptake. This is surprising in view of the fact that we observe autocatalytic behavior of N_2O_5 on ice where much larger HNO_3 concentrations are produced at the surface via reaction 4. It is also important to note that surfaces prepared from initially acidic solutions of nitric acid do not immediately produce the highest N_2O_5 uptake, but rather each solution repeats an induction period of its own characteristic time. This seems contradictory with the observation of a lower absolute value for γ on the preacidified surfaces. The above observations can be reconciled when we consider the different surface morphologies that might be present during the experiments on ice versus nitric acid/ice.

The nitric acid/ice surfaces were prepared by freezing solutions containing known concentrations of HNO_3. Previous work on freezing solutions of HCl in water strongly suggest that HCl is excluded from the ice matrix during freezing.[32,33] For example, in recent experiments on rapidly frozen solutions of HCl/ice, it was found that essentially all of the HCl is found in the grain boundaries of the resulting polycrystalline ice.[32] The same has been suggested for freezing solutions of nitric acid.[29] In this case, one would expect relatively pure regions of ice, with eutectic

---

(32) Wolff, E. W.; Mulvaney, R. *Geophys. Res. Lett.* **1989**, *16*, 487.
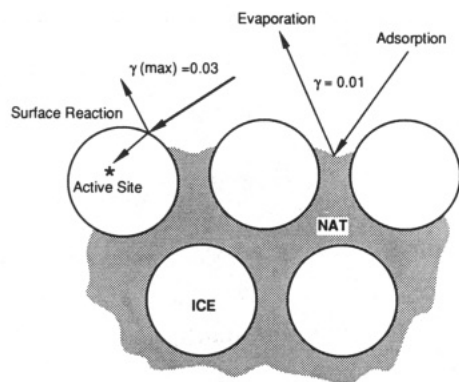(33) Hanson, D.; Mauersberger, K. *J. Phys. Chem.*, in press.

Figure 5. Schematic diagram of possible N_2O_5 interactions on a mixed solid formed from freezing solutions containing nitric acid and water.

compositions such as NAT to be present in the grain boundaries.

An example of what might happen when N_2O_5 encounters such an ice solid with NAT at the grain boundaries is illustrated schematically in Figure 5. The present results indicate that the uptake efficiency of N_2O_5 on NAT is less than that on ice. Thus, any N_2O_5 molecules first encountering the NAT portion of the surface may be more likely to evaporate than molecules first encountering the ice portion of the solid. Thus, the overall uptake efficiency would be reduced on a mixed acid surface relative to a pure ice surface. Note, however, that autocatalytic behavior might still be observed because the reaction on the relatively pure ice portions of the mixed surfaces should behave similarly to pure ice. Detailed modeling studies which include reactions such as those in Table I plus steps that account for surface diffusion and autocatalytic reaction are needed in order to determine whether the above picture can quantitatively account for the observed data. Such studies are currently underway.

Atmospheric Relevance. The present studies were performed on polycrystalline bulk ice samples and vapor-deposited film ice samples. The vapor-deposited films may also be polycrystalline, but with thicknesses on the order of microns. Other laboratory studies have shown that rapidly frozen polycrystalline ice is composed of many single crystals with sizes in the range of 10–20 μm, separated by grain boundaries.[32] The form of ice in the atmosphere is not well known. Ice particles with sizes in the micron range form in the atmosphere by condensation on preexisting particles. These resulting ice particles may be es-

sentially single crystals. Care must therefore be used in extrapolating the present polycrystalline results to ice that would be found in the atmosphere. Nonetheless, we may draw some useful conclusions about the heterogeneous reaction of N_2O_5 on ice and NAT from the present work.

The measured values for the uptake efficiencies rely on knowledge of the surface area that is exposed to gaseous N_2O_5. In the present work, we observe similar values for γ on film and bulk ice and for γ on film and bulk NAT. Because the total microscopic surface areas are clearly very different for these two types of solids, we believe that the gaseous N_2O_5 does not sample the entire microscopic surface area. Adsorbed N_2O_5 may however sample more than the geometric surface area via surface diffusion or diffusion along grain boundaries.

The uptake efficiencies measured in the present work suggest that the reaction of N_2O_5 on both ice and NAT is quite efficient. NAT surfaces appear to be somewhat less reactive than ice surfaces. However, for very short exposure times, <50 s, the uptake efficiency for N_2O_5 on ice is actually smaller than on NAT. Because the reaction on ice appears to be autocatalytic, this trend reverses itself for longer exposures. Thus, the reactivity of N_2O_5 on NAT may actually be higher than on very pure ice. The relatively high reactivity of N_2O_5 on NAT surfaces could be important in the Arctic stratosphere where temperatures favor NAT formation over ice formation. Modeling studies have indicated that reaction efficiencies >0.001 make reaction 4 an important source of HNO_3 in the northern winter stratosphere.[14] The present study suggests that reaction 4 proceeds faster than this limit on both acid-doped ice and NAT surfaces in the laboratory.

Finally, it is important to note that the N_2O_5 fluxes used in the present experiment are much larger than those found in the atmosphere. Thus, the changes we observe on the seconds time scale would occur on a much longer time scale in the atmosphere. It is thus unlikely that N_2O_5 reaction would alter the composition of atmospheric particles to nearly the extent observed in the present work.

Registry No. N_2O_5, 10102-03-1; H_2O, 7732-18-5; $HNO_3\cdot3H_2O$, 13444-83-2.